[9]Straka, W. A., and Hemsch, M. J., "Effect of Fuselage on Delta Wing Vortex Breakdown," *Journal of Aircraft*, Vol. 31, No. 4, 1994, pp. 1002–1005.

[10]Ericsson, L. E., "Comment on 'Effect of Fuselage on Delta Wing Vortex Breakdown,'" *Journal of Aircraft*, Vol. 31, No. 4, 1994, pp. 1006, 1007.

[11]Lambourne, N. C., and Bryer, D. W., "The Bursting of Leading-Edge Vortices—Some Observations and Discussion of the Phenomenon," R&M 3282, Aerodynamic Research Council, England, U.K., April 1961.

[12]Ericsson, L. E., "Further Analysis of Fuselage Effects on Delta Wing Aerodynamics," AIAA Paper 2000-0981, Jan. 2000.

[13]Hanff, E. S., and Jenkins, S. B., "Large Amplitude High-Rate Roll Experiments on a Delta and Double Delta Wing," AIAA Paper 90-0224, Jan. 1990.

[14]Lowson, M. V., and Riley, A. J., "Vortex Breakdown Control by Delta Wing Geometry," *Journal of Aircraft*, Vol. 32, No. 4, 1995, pp. 832–838.

[15]Arena, A. S., Jr., and Nelson, R. C., "Experimental Investigations on Limit Cycle Wing Rock of Slender Wings," *Journal of Aircraft*, Vol. 31, No. 5, 1994, pp. 1148–1155.

[16]Arena, A. S., Jr., and Nelson, R. C., "The Effect of Asymmetric Vortex Wake Characteristics on Slender Delta Wing Undergoing Wing Rock Motion," AIAA Paper 89-3348, Aug. 1989.

[17]Jun, Y. W., and Nelson, R. C., "Leading-Edge Vortex Dynamics on a Delta Wing Undergoing Wing Rock Motion," AIAA Paper 87-0332, Jan. 1987.

[18]Lowson, M. V., "Some Experiments with Vortex Breakdown," *Journal of the Royal Aeronautical Society*, Vol. 68, May 1964, pp. 343–346.

[19]Ericsson, L. E., and Hanff, E. S., "Further Analysis of High-Rate Rolling Experiments of a 65-Degree Delta Wing," *Journal of Aircraft*, Vol. 31, No. 6, 1994, pp. 1350–1357.

[20]Harvey, J. K., "A Study of the Flow Field Associated with a Steadily Rolling Slender Delta Wing," *Journal of the Royal Aeronautical Society*, Vol. 68, Feb. 1964, pp. 106–110.

[21]Ericsson, L. E., and Beyers, M. E., "Ground Facility Interference Effects on Slender Vehicle Unsteady Aerodynamics," *Journal of Aircraft*, Vol. 33, No. 1, 1996, pp. 117–124.

Elastomeric Damper Model and Limit Cycle Oscillation in Bearingless Helicopter Rotor Blade

G. Pohit,* C. Venkatesan,† and A. K. Mallik‡
Indian Institute of Technology, Kanpur, U.P. 208 016, India

I. Introduction

WITH the advancement in technology, development of a mechanically simple yet efficient rotor blade system has resulted in the design of a bearingless blade and hub configuration.[1] A schematic diagram of a bearingless rotor blade is shown in Fig. 1. In this rotor system (Fig. 1), the blade is attached to the hub through a flexbeam that is designed to provide the required stiffness in the flap and lag bending deformation of the blade, but that is highly flexible in torsion. Surrounding the flexbeam, there is a stiff cuff denoted as the torque tube, which is attached to the blade–flexbeam junction at the outboard end and to a pitch link at the inboard end, as shown in Fig. 1. The pitch control of the blade is achieved by rotating the torque tube through the up/down movement of the point P, which, in turn, twists the flexbeam. An elastomeric damper is placed between the torque tube and flexbeam to provide adequate lag damping. It also acts as a spacer between the torque tube and the flexbeam. Though a bearingless rotor is mechanically simple, its dynamic analysis becomes complicated due to the presence of a multiple load path and a nonlinear elastomeric damper.

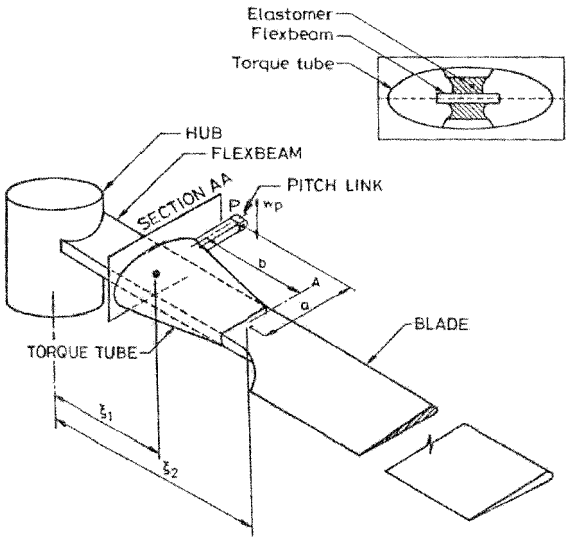

Fig. 1 Bearingless rotor blade with pitch link at the leading edge.

The nonlinear dynamic characteristics of the elastomer are usually represented by the variation of in-phase stiffness (stiffness) and quadrature stiffness (damping) as a function of amplitude. The experimental results of a single frequency bench test of different elastomeric lag dampers are available in Refs. 2–4. All of these data indicate that both the in-phase stiffness K' and the quadrature stiffness K'' decrease as the amplitude of motion increases. The variation of loss tangent or loss factor η with amplitude is also shown in Ref. 3. Loss tangent is generally defined as the ratio of K'' and K'. In a recent publication, Kunz[5] also indicated similar types of stiffness and damping characteristics of the elastomer with respect to the amplitude of motion.

There are several linear models to describe the mechanical behavior of visco-elastic materials, for example, anelastic displacement fields (ADF) have been used in Ref. 6. Smith et al.[7] extended the method of ADF to include the nonlinearities and temperature effects. The nonlinear characteristics of elastomers have been analyzed in detail in several recent publications.[8–12] Some of the recent studies have focused on the phenomenon of the limit-cycle behavior of bearingless rotor blades due to the elastomer nonlinearity. In Ref. 11, Gandhi and Chopra proposed a nonlinear viscoelastic model for the elastomer in which the damping element is linear. The model shows a rapid decrease in damping coefficient at very low amplitudes of oscillation, but its value is always positive. With this elastomeric damper, they showed a limit-cycle oscillation for an autonomous system representing the isolated lag dynamics of a blade. Ormiston et al.[13] considered an elastomer model in which the damping force was assumed to be proportional to a linear combination of different powers of velocity (powers of 0.5, 1, 2, and 3). Using this nonlinear elastomer model, they showed the presence of limit-cycle oscillation for both hingeless and bearingless rotor blade configurations. It was also pointed out that there was no limit cycle when the elastomer damping is taken as linear. The hover air-resonance analysis and wind-tunnel test by Panda and Mychalowycz[1] also indicated that nonlinearities in stiffness and damping characteristics of the elastomer seem to have a significant influence on the limit-cycle oscillations. When they used a fluidlastic damper having linear characteristics, no limit-cycle oscillation was observed.

The objective of the present Note is to analyze the relation between elastomer modeling and limit-cycle oscillation. The example problem chosen to address this is the transient response behavior of an isolated bearingless rotor blade undergoing coupled flap–lag–torsional deformation under a hovering condition. The

Received 18 July 1999; revision received 13 June 2000; accepted for publication 17 June 2000.

*Graduate Student, Department of Mechanical Engineering.

†Professor, Department of Aerospace Engineering. Senior Member AIAA.

‡Professor, Department of Mechanical Engineering.

response of the blade is evaluated for a given step control pitch input with different elastomer models representing the same experimental data.

II. Limit Cycle

The theorem on the existence of a limit cycle[14] says that for the equation

$$\ddot{x} + f(x)\dot{x} + g(x) = 0 \tag{1}$$

to exhibit a limit cycle, $f(x)$ must be positive when $|x|$ is large and negative when $|x|$ is small and g is such that, in the absence of the damping term $f(x)\dot{x}$, a periodic solution is expected for small x. In Van der Pol's equation

$$\ddot{x} + e(x^2 - 1)\dot{x} + x = 0, \qquad e > 0 \tag{2}$$

that is, the damping coefficient becomes negative in the strip $|x| < 1$ and positive for $|x| > 1$. Therefore, the phenomenon of a stable limit-cycle oscillation in an autonomous system requires that the damping coefficient must change sign during one cycle.

III. Formulation of Elastomer Model

Because experimental data are used in developing an analytical spring-damper model for the elastomer, there is a scope for formulating many different types of models. In this Note, two different models of the elastomer are proposed as shown in Fig. 2. First, the elastomer is modeled (model 1) as a parallel combination of a nonlinear spring, a coulomb damper, and a hysteretic damping. The second model (model 2) consists of a nonlinear spring, a coulomb damping element, and a Rayleigh-type hysteretic damping element.

The experimental results[2–4] of an elastomeric lag damper show that both in-phase (K') and quadrature (K'') stiffnesses decrease as the amplitude of motion decreases, but that neither of them display any significant dependence on frequency within the range of interest (3.3–6.8 Hz) as shown in Ref. 4. The reason for choosing a coulomb damper is that the damping force is very high at low amplitude. In addition, coulomb and hysteretic dampers provide damping forces that are independent of frequency. This type of idealization differs from the model proposed by Gandhi and Chopra[11] in the sense that their model has a viscous damping element. The constitutive differential equation of the elastomer model under harmonic loading for model 1 can then be written as

$$K_1 x - K_3 x^3 + K_5 X^5 - K_7 X^7 + F\,\mathrm{sgn}|\dot{x}| + (h_1/\omega)\dot{x} = D_0 \sin \omega t \tag{3}$$

and that for model 2 can be written as

$$K_1 x - K_3 x^3 - K_5 X^5 - K_7 X^7 + F\,\mathrm{sgn}|\dot{x}| + \left(h_3/\omega^3\right)\dot{x}^3 - (h_1/\omega)\dot{x} = D_0 \sin \omega t \tag{4}$$

where D_0 is the amplitude of the excitation force and K_1, K_3, K_5, K_7, F, h_1, and h_3 are system parameters of the elastomer.

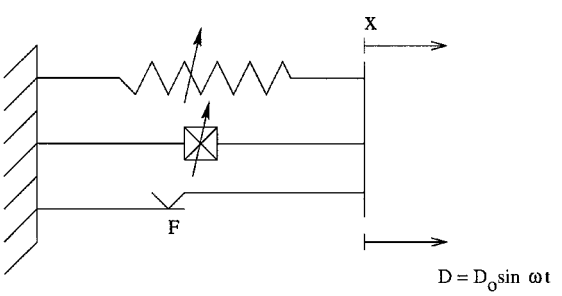

Fig. 2 Elastomer model.

When we assume a harmonic motion and follow the procedure mentioned in Refs. 11 and 15, the in-phase stiffness K' and the quadrature K'' for model 1 can be obtained as

$$K' = K_1 - \tfrac{3}{4}K_3X^2 + \tfrac{5}{8}K_5X^4 - \tfrac{1}{2}K_7X^6 \tag{5}$$

$$K'' = (4F/\pi X) + h_1 \tag{6}$$

and that for model 2 can be obtained as

$$K' = K_1 - \tfrac{3}{4}K_3X^2 + \tfrac{5}{8}K_5X^4 - \tfrac{1}{2}K_7X^6 \tag{7}$$

$$K'' = (4F/\pi X) + \tfrac{3}{4}h_3X^2 - h_1 \tag{8}$$

Note that in model 2, the term corresponding to Rayleigh-type hysteretic damping changes sign with varying amplitude.

IV. Equations of Motion and Solution Procedure

The transient response analysis of a bearingless rotor blade requires the formulation of the aeroelastic equations of motion representing coupled axial, flap, lag, and torsional motion of the blade, including the nonlinear elastomer. Based on the assumption of an Euler–Bernoulli beam, the strain and kinetic energy expressions of the blade are obtained. During blade deformation, the elastomer provides constraints in flap, lag, and torsional deformation of the blade. Because elastomer data are available[2,3] only for the lag mode, in this study, following the approach of Ormistron et al.,[13] the elastomer is represented by a very stiff linear spring in flap mode. In the lag mode, the elastomer is represented by both models 1 and 2. The effect of elastomer is not considered in the torsional mode.

The aerodynamic forces and moments are treated as external loads acting on the blade. The expressions for aerodynamic loads are derived by an implicit formulation. The time-varying aerodynamic lift and pitching moment, acting on a typical cross section of the blade are evaluated based on Greenberg's extension of Theodorsen's theory. Because the present study addresses the transient response of the rotor blade, a time-varying inflow model, which is represented by dynamic inflow model,[16] has to be considered. The equations of motion are derived using Hamilton's principle. The details of the derivation can be found in Ref. 17.

Following the assumed mode method, the flap, lag, and torsional equations of motion have been derived. These equations are nonlinear, coupled ordinary differential equations. The transient response of the blade to a step control pitch input is obtained by simultaneously solving the nonlinear coupled equations and the inflow equation by a numerical integration routine based on a Runge–Kutta–Marson algorithm.

V. Results and Discussion

The parameters for the elastomer models 1 and 2 are obtained by an error minimization technique, and they are given in Table 1. The experimental data of the elastomer are taken from Ref. 4. The blade data are given in Table 2. The nondimensional uncoupled natural

Table 1 System parameters of the elastomeric damper models 1 and 2

System parameter	Model 1	Model 2
K_1, N/m	2.673989×10^6	2.673989×10^6
K_3, N/m^3	1.315287×10^{12}	1.315287×10^{12}
K_5, N/m^5	3.519586×10^{17}	3.519586×10^{17}
K_7, N/m^7	3.176266×10^{22}	3.176266×10^{22}
F, N	4.797347×10^2	8.45909×10^2
h, N/m	4.569120×10^5	—
h_1, N/m	—	1.44619×10^5
h_3, N/m^3	—	7.06419×10^{10}

Table 2 Input data for transient response analysis[a,b]

Parameter	Value
Lock number, γ	5
Blade semi chord, b_1/L	$\pi/20$
Lift curve slope, a_1	2π
Number of blades, N	4
Torsional rigidity, $GJ/m\Omega^2L^4$	0.001473
Flap flexural rigidity, $EI_{\zeta\zeta}/m\Omega^2L^4$	0.0301
Lag flexural rigidity, $EI_{\eta\eta}/m\Omega^2L^4$	0.0106
Moment of inertia, $\mathrm{Im}_{\zeta\zeta}/mL^2$	0.0004
Moment of inertia, $\mathrm{Im}_{\eta\eta}/mL^2$	0.0
$(k_A/k_m)^2$	1.5

[a] $k_A^2 = (EI_{\eta\eta} + EI_{\zeta\zeta})/EA$, $k_m^2 = (\mathrm{Im}_{\eta\eta} + \mathrm{Im}_{\zeta\zeta})/mL^2$.
[b] Offsets of mass center, tension center, and aerodynamic center from the elastic axis are zero.

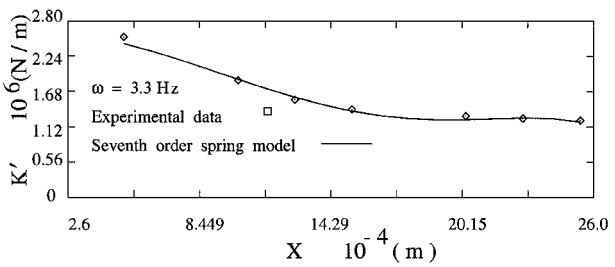

Fig. 3a Variation of K' (in-phase stiffness) with amplitude; ◇, experimental data.

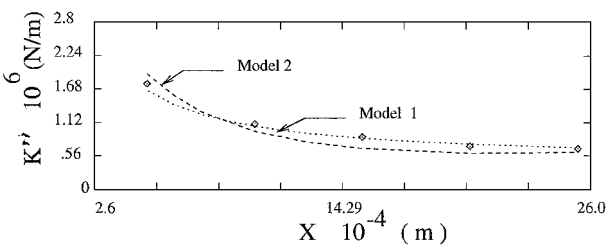

Fig. 3b Variation of K'' (quadrature stiffness) with amplitude; ◇, experimental data (comparison of the experimental data with models 1 and 2).

frequencies of the blade in first lag, first flap, and first torsion modes are 0.732, 1.124, and 3.174, respectively.

Comparison of the experimental data with models 1 and 2 is shown in Fig. 3. It can be seen that both of the models fit the experimental values fairly well in the available range of data. In the absence of experimental data on the hysteresis effects of the elastomer, compare the theoretical hysteresis loops generated for the two elastomer models. Figure 4 shows the hysteresis loops of the two elastomer models, for two different amplitudes of motion. Though both models provide similar loops, the hysteresis loop of model 1 encloses more area than that of model 2, for the same amplitude of motion.

The transient response characteristics of the bearingless rotor blade are obtained by the use of models 1 and 2. The blade and the flexbeam properties are considered to be same due to lack of availability of practical blade data and also for simplicity. Even though uniform properties have been assumed for flexbeam and blade, the natural frequencies of the rotating blade in flap, lag, and torsional modes are representative of a realistic rotor blade configuration.

The response of the blade is evaluated in modal space by considering three modes in flap, two modes in lag, and one mode in torsion. The elastomer and torque tube locations are set at $\xi_1 = 0.10$ and $\xi_2 = 0.25$ (Fig. 1). The pitch link is located at the leading-

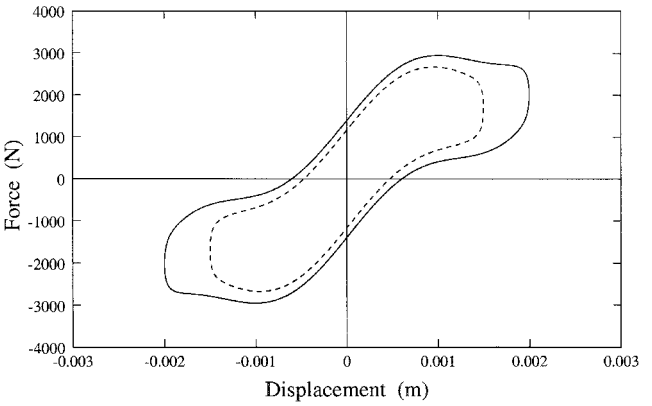

Model 1

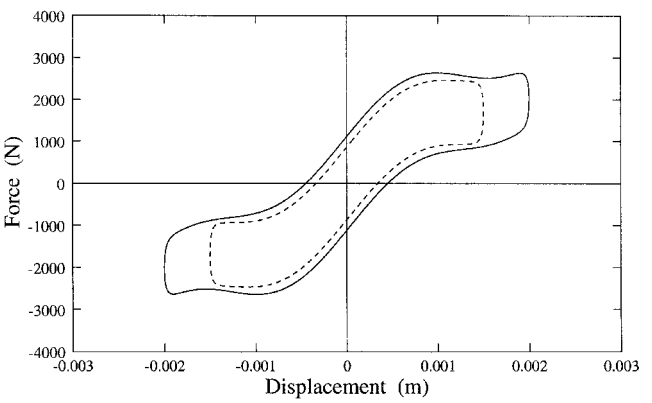

Model 2

Fig. 4 Comparison of the hysteresis curves for different amplitudes of motion; ——, X = 0.002 m and - - - -, X = 0.0015 m.

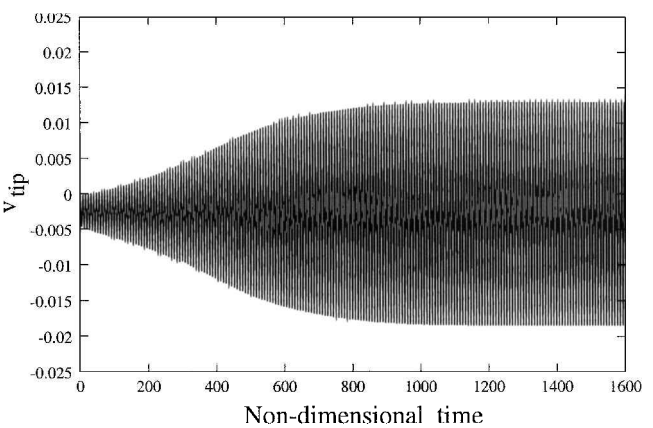

Fig. 5 Transient response in lag mode with model 2 (with aerodynamic loading).

edge side of the blade with $a = 0.03$ and $b = 0.10$. A step control input of $w_P = 0.00361$ (equivalent to a static blade pitch input of 0.12 rad) is applied. All length data are normalized with respect to blade length. Figures 5 and 6 show the transient response in lag mode for the two cases. In the case of model 2 (Fig. 5), it is observed that, within a short time, the lag response settles down to a stable limit-cycle oscillation with a constant amplitude of 0.0145 with a mean value of −0.0035, whereas in the case of model 1 (Fig. 6), the transient response in lag mode settles to steady-state value of −0.0027. The blade responses shown in Figs. 5 and 6 are obtained with the inclusion of aerodynamic loading. The nondimensional frequency of limit-cycle oscillation is found to be 0.58.

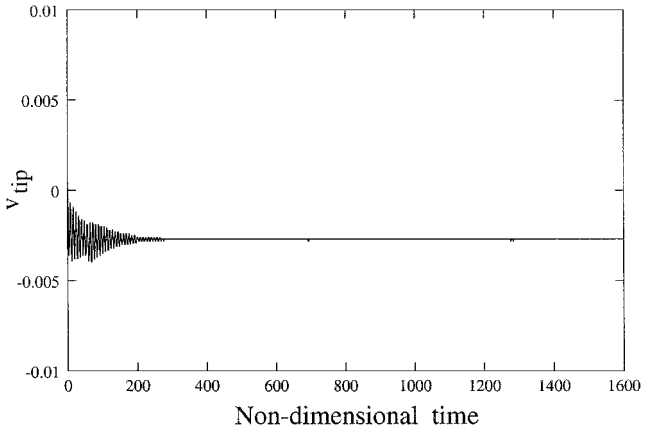

Fig. 6 Transient response in lag mode with model 1 (with aerodynamic loading).

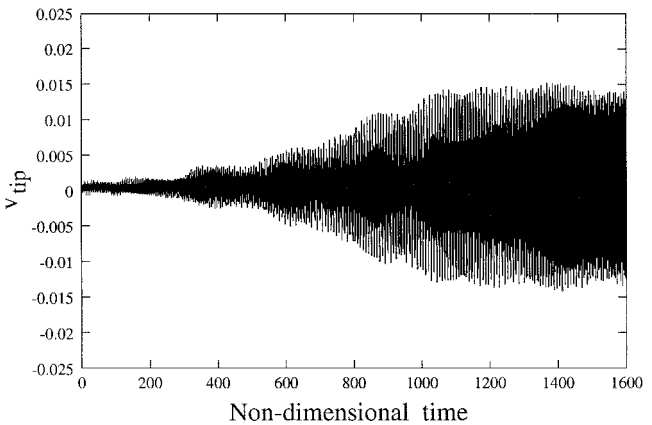

Fig. 7 Transient response in lag mode with model 2 (without aerodynamic loading).

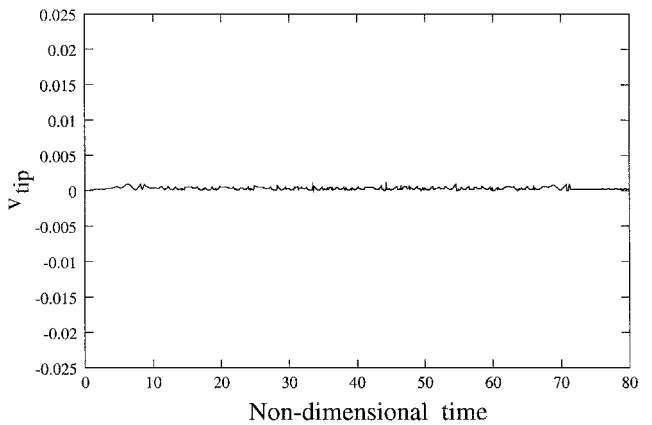

Fig. 8 Transient response in lag mode with model 1 (without aerodynamic loading).

To ensure that the cause of limit cycle is due to the elastomer model and not due to external aerodynamic loading, the transient analysis is also carried out by excluding the aerodynamic effects. For the same set of blade parameters and step control input, the response of the blade is computed. Figures 7 and 8 show the responses in lag mode of the blade with elastomer models 2 and 1, respectively. Whereas the response of model 2 exhibits a limit-cycle oscillation (Fig. 7), no such oscillation is observed for model 1 (Fig. 8). In this case, the frequency of limit-cycle oscillation is observed to be 0.72.

VI. Conclusions

This Note investigates the phenomenon of limit cycle in bearingless rotor blades by studying the transient response of the blade with two different models of elastomer. Even though both elastomer models fit the experimental data fairly well, the response characteristics of the blade exhibit a totally different nature. These results clearly indicate that the phenomenon of limit-cycle oscillation is highly dependent on elastomer model. Hence, care must be exercised in modeling the elastomer.

Acknowledgment

The authors wish to acknowledge financial support from the Structures Panel of the Aeronautics Research and Development Board, India.

References

[1]Panda, B., and Mychalowycz, E., "Aeroelastic Stability Wind Tunnel Testing with Analytical Correlation of the Comanche Bearingless Main Rotor," *Journal of the American Helicopter Society*, Vol. 42, No. 3, 1997, pp. 207–217.

[2]McGuire, D. P., "The Application of Elastomer Lead-Lag Dampers to Helicopter Rotors," Lord Library L2133, Lord Corp., Erie, PA, 1976.

[3]Housmann, G., "Structural Analysis and Design Considerations of Elastomeric Dampers with Viscoelastic Material Behavior," *Twelfth European Rotorcraft Forum*, 1986, pp. 70.1–70.26.

[4]Felker, F., Lau, B., Mclaughlin, S., and Johnson, W., "Nonlinear Behavior of an Elastomeric Lag Damper Undergoing Dual-Frequency Motion and Its Effect on Rotor Dynamics," *Journal of the American Helicopter Society*, Vol. 34, No. 4, 1987, pp. 45–53.

[5]Kunz, D. L. "Influence of Elastomeric Damper Modeling on the Dynamic Response of Helicopter Rotors," *AIAA Journal*, Vol. 35, No. 2, 1997, pp. 349–354.

[6]Lesieutre, G. A., and Bianchini, E., "Time-Domain Modeling of Linear Visco-Elasticity Using Anelastic Displacement Fields," *Journal of Vibration and Acoustics*, Vol. 117, No. 4, 1995, pp. 424–430.

[7]Smith, E. C., Beale, M. R., Govindswamy, K., Vascsineci, M. J., and Lesieutre, G. A., "Formulation and Validation of a Finite Element Model for Elastomeric Lag Dampers," *51st Annual Forum of the American Helicopter Society*, 1995, pp. 1101–1116.

[8]Byers, L. K., Lesieutre, G. A., Smith, E. C., and Beale, M. R., "Transient Behavior of Elastomeric Damper and Bearing Materials," AIAA Paper 96-1218, April 1996.

[9]Ruhl, L. E., Lesieutre, G. A., Brackbill, C. R., and Smith, E. C., "Thermomechanical Modeling of Elastomeric Damper Materials," AIAA Paper 99-1221, April 1999.

[10]Brackbill, C. R., Lesieutre, G. A., Ruhl, L. E., and Smith, E. C., "Characterization and Modeling of the Low Strain Amplitude and Frequency Dependent Behavior of Elastomeric Damper Materials," AIAA Paper 98-1845, April 1998.

[11]Gandhi, F., and Chopra, I., "Analysis of Bearingless Main Rotor Dynamics with the Inclusion of an Improved Time Domain Nonlinear Elastomeric Damper Model," *Journal of the American Helicopter Society*, Vol. 41, No. 3, 1996, pp. 267–277.

[12]Potter, J. L., McGuire, D. P., and Brubaker, E. L., "Elastomers + Fluid + Electronics = Improved Comfort and Reliability for Aircraft," *International Exhibition Cum Seminar on Helicopter Development and Utilisation in South Asia-Pacific*, 1995, pp. 6.3-1–6.3-19.

[13]Ormiston, R. A., Saberi, H., and Anastassiades, T., "Application of 2GCHAS to the Investigation of Aeromechanical Stability of Hingeless Rotor Helicopters," *51st Forum of the American Helicopter Society*, 1995, pp. 1132–1155.

[14]Jordon, D. W., and Smith, P., *Nonlinear Ordinary Differential Equations*, Clarendon Press, Oxford, England, U.K., 1999, pp. 408–414.

[15]Pohit, G., Mallik, A. K., and Venkatesan, C., "Free Out-of-Plane Vibration of Rotating Beam with Non-Linear Elastomeric Constraints," *Journal of Sound and Vibration*, Vol. 220, No. 1, 1999, pp. 1–25.

[16]Pitt, D. M., and Peters, D. A., "Theoretical Prediction of Dynamic Inflow Derivatives," *Vertica*, Vol. 5, No. 1, 1981, pp. 21–34.

[17]Pohit, G., "Dynamics of a Bearingless Helicopter Rotor Blade with a Non-Linear Elastomeric Constraint," Ph.D. Thesis, Dept. of Mechanical Engineering, Indian Inst. of Technology, Kanpur, India, Feb. 1999.